Organic Matter Loading Modifies the Microbial Community Responsible for Nitrogen Loss in Estuarine Sediments

Organic matter loading modifies the microbial community responsible for nitrogen loss in estuarine sediments

Andrew R. Babbin[a,b]#, Amal Jayakumar[a], Bess B. Ward[a]

Department of Geosciences, Princeton University, Princeton, NJ, USA[a];

Department of Civil & Environmental Engineering, MIT, Cambridge, MA, USA[b]

#Correspondence to Andrew R. Babbin, babbin@mit.edu.

Keywords: anammox, denitrification, nitrogen cycle, marine sediments

Abstract

Coastal marine sediments, as locations of substantial fixed nitrogen loss, are very important to the nitrogen budget and to the primary productivity of the oceans. Coastal sediment systems are also highly dynamic and subject to periodic natural and anthropogenic organic substrate additions. The response to organic matter by the microbial community involved in nitrogen loss processes was evaluated using mesocosms of Chesapeake Bay sediments. Over the course of a 50-day incubation, rates of anammox and denitrification were measured weekly using ^{15}N tracer incubations, and samples were collected for genetic analysis. Rates of both nitrogen loss processes and gene abundances associated with them corresponded loosely, probably because heterogeneities in sediments obscured a clear relationship. The rates of denitrification were stimulated more, and the fraction of nitrogen loss attributed to anammox slightly reduced, by the higher organic matter addition. Furthermore, the large organic matter pulse drove a significant and rapid shift in the denitrifier community composition as determined using a *nirS* microarray, indicating the diversity of these organisms plays an essential role in responding to anthropogenic inputs. We also suggest that the proportion of nitrogen loss due to anammox in these coastal estuarine sediments may be underestimated due to temporal dynamics as well as from methodological artifacts related to conventional sediment slurry incubation approaches.

Introduction

Coastal and estuarine sediments are environments of intense loss of fixed nitrogen through the microbial processes of denitrification and anaerobic ammonium oxidation (anammox). Globally, these areas can account for up to three-quarters of the fixed nitrogen lost from the marine system [1–3]. Direct measurement of the fixed nitrogen loss rates is difficult,

however, because of significant spatial and temporal heterogeneities characteristic of sediments. For instance, oxic or anoxic microsites [4] and an uneven distribution of organic matter create pockets of reduced or enhanced nitrogen cycling, while episodic bloom-derived settling events of organic matter onto sediment beds can lead to spikes in nitrogen loss rates [5]. How the microbial community of denitrifiers and anammox bacteria responds to this sudden input of organic matter in terms of biological rates and community composition is a crucial question in better understanding these dynamic and climatically relevant sediment systems.

Increased fixed nitrogen levels are typically associated with coastal estuarine systems such as Chesapeake Bay, where higher concentrations of ammonium and urea are measured following spring storm events [6–8]. During these periods, fertilizer applied to croplands runs off into the tidal estuary, and causes phytoplankton blooms which in turn deposit on the sediment bed. Aquaculture in cages or pens also contributes high organic loading in some systems. Additionally, discharge of sewage, either by inadequate treatment facilities or through combined sewage overflow, is another avenue by which nitrogen is directly injected into the coastal environment. These transient pulses consist of high concentrations of ammonium, nitrate, and labile particulate organic matter [6, 9, 10]. The link between these events and the microbial community that consumes this nitrogen is therefore key in understanding the amplitude of the response of the coastal system to anthropogenically-derived nitrogen.

Denitrification, anammox and dissimilatory nitrate reduction to ammonium (DNRA) are all involved in nitrogen removal from sediments. The major consumption of fixed nitrogen in natural estuarine sediments is denitrification [11, 12], the heterotrophic stepwise reduction of nitrate or nitrite to nitrous oxide and dinitrogen gas via a series of reductase enzymes. Of the multiple enzymes in this sequence, nitrite reductase, which converts nitrite to nitric oxide is the

most critical in that it is the one that leads rapidly to loss of fixed nitrogen from the environment. This enzyme is encoded by *nirS*, a diverse gene commonly found in denitrifiers [13], or by *nirK*, which encodes a metabolically equivalent but structurally distinct enzyme. In Chesapeake Bay and other estuarine systems, however, *nirK* has been difficult to detect and is consistently found at much lower copy numbers [14–18], making *nirS* the more useful functional biomarker gene for denitrification in Chesapeake Bay. In estuarine environments, much of the organic matter, which is required for denitrification, is highly refractory [19], with a C/N ratio > 9 and not readily solubilized. The anthropogenic addition of labile easily-solubilized organic molecules may therefore enhance denitrification rates when nitrate is present [20–22].

Anammox too removes fixed nitrogen from certain sediment environments [23, 24]. Still, anammox was minimal in trout aquaculture settlement ponds [25] and a rare but significant contribution in shrimp aquaculture ponds [26]. It was also reported to be a minor nitrogen loss process in three U.S. east coast estuaries, Chesapeake Bay [11], Cape Fear [27], and Providence River [28]. These low rates imply a limited significance for DNRA-coupled nitrogen loss whereby anammox consumes ammonium provided in situ by DNRA. Anammox, an autotrophic process by which ammonium is oxidized anaerobically using nitrite as an electron acceptor, is constrained by similar dissolved oxygen and DIN controls as denitrification despite fundamentally different metabolisms. Anammox requires both reduced (ammonium) and oxidized (nitrite) forms of nitrogen, which do not usually co-occur in space or time due to (1) the ability of nitrification to aerobically oxidize ammonium even with limited amounts of oxygen [29–31], and (2) the reduction of nitrite via denitrification using high C/N organic matter substrate reserves in sediments. Given a large enough pulse of reduced inorganic (i.e. ammonium) or organic nitrogen, however, anammox may be able to utilize these conditions to

couple with nitrification and/or heterotrophic nitrate reduction to remove ammonium rapidly [32]. In this sense, both anammox and denitrification can be controlled by the same organic and inorganic nitrogen substrates, and can be stimulated by their injection into the estuarine system.

Ammonium is the critical link in constraining rates of sedimentary anammox and denitrification because it does not accumulate sufficiently in the anoxic depth layers of active nitrogen loss [33, 34]. Therefore, barring physical transport, mass balance on ammonium implies that anammox consuming NH_4^+ and denitrification producing it should occur in specific ratios set by the stoichiometry of organic matter fueling nitrate reduction and denitrification. Analogous stoichiometry-dependent coupling has been shown in the anoxic water column [35], and is also likely important in anoxic sediments [5, 36]. For instance, if the material reaching the sediments is of average marine phytoplankton composition (C/N = 6.6), anammox should account for 29% of the fixed nitrogen loss [37]. This anammox proportion, however, should vary with organic nitrogen content relative to carbon fueling the microbial community: more nitrogen corresponds to higher amounts of anammox relative to denitrification. Additional allochthonous NH_4^+ supplied through runoff or from remineralization in deeper sediments via processes such as sulfate reduction could further amplify the anammox contribution, as observed in deep sea sediments off the Washington margin [24].

We used an incubation approach in order to reduce natural variability and to test the effect of organic matter on the rates of fixed nitrogen loss in the absence of other variables. Using replicate sediment mesocosms, we controlled the supply of organic and inorganic nutrients. Although the mesocosms do not simulate the actual system response to a bloom setting event or pulses of inorganic nutrients, they allow us to investigate the mechanisms and directions of change that might occur in the natural estuarine system. We measured the time dependence of

nitrogen loss rates and gene abundances for anammox (*16S rRNA*) and denitrification (*nirS* functional gene) following an injection of ammonium, nitrate, and two levels of organic matter. We further used the diversity of the *nirS* gene as determined from a microarray analysis to quantify the denitrifier community response to the organic substrate pulse at two different levels.

Materials and Methods

Mesocosm design

The mesocosm experiments, as previously described by Babbin and Ward [5], were seeded with sediments and site water from the lower Choptank River in the Chesapeake Bay estuary (station CT2, 38°37.191′ N 76°08.061′ W, station depth = 7.9, salinity = 14) collected in November 2009. Briefly, homogenized sediments were divided into four replicate containers (cross-section of 40 cm × 25 cm) forming a layer ~2.5 cm in thickness, and overlain with ~18.5 cm of site water. The sediments were pre-incubated for six months to remove any preexisting labile substrates before nitrate and ammonium in the overlying water were restored to near-original concentrations, and organic matter in the form of commercially available fish food (C/N = 4.2; Tetrafin, Blacksburg, VA) was applied to the surface of the sediments. Two of the mesocosms (L1 and L2) received 0.4 mg cm^{-2} organic matter, and two (H1 and H2) received a 10-fold higher addition of 4.0 mg cm^{-2}. The level of organic matter addition was chosen to provide a large signal in the biogeochemical and microbial community response, and similar to previous mesocosm studies, e.g., [38, 39]. The organic matter amendment was raked across the surface of the sediments in order to seed the approximate depth zone (upper few millimeters) of the active nitrogen cycle and to mimic a natural deposition event such as might occur after a phytoplankton bloom.

The mesocosms were incubated for seven weeks in the dark at room temperature following the organic matter additions. The overlying water was aerated and mixed by gently bubbling with air, which also prevented the build up of sulfide (sulfide was never sensed over the course of the incubation). Overlying water was sampled daily for dissolved inorganic nitrogen (DIN), measured using standard techniques [5]. Periodically, the mesocosm sediments were also sampled for instantaneous rate experiments and DNA by coring an entire 2.5 cm sediment plug, homogenizing, and aliquoting into incubation vials for isotope labeling experiments (rate measurements) or Nalgene cryovials and frozen at –80 °C (DNA) [17].

Rate experiments

Three full-depth sediment cores (90% porosity) were collected from each mesocosm using a syringe into a 20 mL vial. The vials were then homogenized in an Argon-flushed glove bag, and 1.5 mL subsamples were aliquoted into 5.9 mL Exetainers (Labco, UK), similar to previous studies [11, 40]. Concentrated stocks of [^{15}N]-labeled NH_4^+ or NO_2^- were added (final amendment of 4 nmol N), and the vials capped. The Exetainers were vortexed briefly to distribute the tracer, and flushed on a gas purging manifold at 5 psi of Argon for 5 minutes. Triplicate vials were killed with 100 µL 50% (w/v) $ZnCl_2$ solution at time points of 0 and 30 min. Production of labeled [^{15}N]-N_2 gas from the ammonium and nitrite treatments were measured on a Delta V Plus IRMS (ThermoScientific) at the UC Davis Stable Isotope Facility. The incubation time of 30 minutes was determined as appropriate for linear production of N_2 from previous experiments in Chesapeake Bay [11].

After analysis for gases, 2 mL of 2 mol L^{-1} KCl solution was added to the sediment slurry, and vials shaken on a reciprocal shaker for 12 hours at 100 rpm. The slurries were then

centrifuged (2000×g, 5 min) and supernatant collected and frozen until analysis. NH_4^+ was measured using fluorometry after conversion with orthophthaldialdehyde [41] and NO_2^- with standard spectrophotometric techniques [42]. These concentrations, generally below detection (data not shown), were used to determine fraction of substrate labeled to calculate the nitrogen loss rates (e.g., 11, 31).

DNA extraction and quantitative PCR amplification

DNA from mesocosms L1 and H1 was extracted in duplicate from 0.5 g (wet weight) sediment aliquots (temperature = 25 °C, pH = 8, salinity = 14) using the MoBio PowerSoil® DNA Isolation Kit (MoBio Laboratories, Carlsbad, CA) following manufacturer's protocols. Duplicate extracts were then pooled for qPCR analysis. Methods of qPCR using SYBR Green for *nirS* and anammox *16S rRNA* genes, and the standardization and verification of specificity for qPCR assays were performed as described previously [43]. The efficiency of the qPCR reactions was calculated using the slopes of the standard curves, and was 77% for anammox *16S rRNA* assay and 107% for *nirS* assay. The amplified products were visualized after electrophoresis in 1% agarose gels stained with ethidium bromide. Standards for PCR quantification of each fragment were prepared by amplifying a constructed plasmid containing the respective gene fragment, followed by quantification and serial dilution.

Assays of each gene for all four samples were carried out within a single assay plate [44]. Each assay included triplicates of the no template controls, no primer control, five (*nirS*) or seven (anammox *16S rRNA*) standards, and triplicates of known quantity of the environmental DNA samples (20 – 25 ng). DNA was quantified using PicoGreen fluorescence (Molecular Probes, Eugene, OR) calibrated with several dilutions of phage lambda standards and qPCR was

performed using a Stratagene MX3000P (Agilent Technologies, La Jolla, CA). Automatic analysis settings were used to determine the threshold cycle (Ct) values.

nirS microarray analysis

The array (BC014) was developed with the archetype array approach described and conducted previously [45, 46] with 90-mer oligonucleotide probes. Each probe consisted of a *nirS*-specific 70-mer region and a 20-mer control region (5′-GTACTACTAGCCTAGGCTAG-3′) bound to a glass slide. The design and spotting of the probes has been described previously [47, 48]. BC014 contains 164 *nirS* archetype probes representing ~2000 sequences from a range of environments, including both sediments and oxygen deficient zone water columns, that were publicly available in November 2009 when the array was designed (the probe accession numbers and sequences are described elsewhere) [46]. The probes differ from each other by ~15% sequence identity, the level at which cross hybridization is insignificant [47].

Array analysis was performed as described previously [46, 49] with some modifications. Triplicate qPCR *nirS* gene fragment amplicons were pooled, gel purified, and labeled with amino-allyl-dUTP (Life Technologies) during linear amplification using random octamers and a Klenow polymerase (Invitrogen). The reaction contained 3.9 mmol L^{-1} d(AGC)TP, 0.4 mmol L^{-1} dTTP, and 4.8 mmol L^{-1} dUaa, and was carried out at 37 °C for 3 hours. The Klenow product was purified by precipitation and conjugated with Cy3 dye. The Cy3-labelled target (200 ng) was combined with hybridization buffer (Agilent) and 0.25 pmol of a Cy5-labelled complementary 20-mer standard oligonucleotide then incubated at 95 °C for 5 min before being cooled to room temperature. Targets were hybridized to duplicate or triplicate arrays by overnight incubation at 64 °C and washed. The arrays were scanned with a laser scanner (Molecular Devices 4300) and

analyzed with Gene Pix Pro 6.0 software (Molecular Devices). Quantification of hybridization signals was performed as described previously [46] including the following quality controls for signal reproducibility. For each channel, i.e. 532 nm (Cy3) and 635 nm (Cy5), the average background fluorescence was recalculated after excluding background fluorescence values greater than the upper whisker of all of the background fluorescences. This limit was defined as the 75th percentile plus 1.5 times the interquartile range. Such a filtering process was applied within each block on a microarray to account for variability in background fluorescence between blocks within an array.

Then a normalized fluorescence ratio (FRn) for each archetype was calculated by dividing the fluorescence signal of the archetype by the highest fluorescence signal within the same array, and the FRn of each archetype from the replicate arrays was averaged. The relative fluorescence ratio (RFR) of each archetype was calculated as the contribution of FRn of the archetype to the cumulative sum of FRn of all *nir*S archetypes on the array and averaged for replicate arrays from each sample. The original array data are available at Gene Expression Omnibus (http://www.ncbi.nlm.nih.gov/projects/geo/) at the National Center for Biotechnology Information under GEO Accession Number GSE65430.

The array data were analyzed using the 'vegan' package in R (http://www.R-project.org) [50]. Archetypes contributing less than 1% of the total signal in all samples were removed from further analysis. RFR values $\geq$ 1% were arcsine–square root transformed to normalize the proportional data. Environmental data were square root transformed and then standardized around zero (decostand in vegan). The transformed data were used in all diversity and correlation analyses according to Borcard et al. [50].

Results

Mesocosm DIN concentrations over time

The progression of the different DIN species – NH_4^+, NO_2^-, and NO_3^- – measured in the water overlying the sediments in the mesocosms has been published in detail previously [5]. To provide context for the experimental data presented here, however, the DIN results are summarized. The two levels of organic matter addition stimulated different magnitudes and timings of mineralization, DIN accumulation, associated nitrification and nitrogen loss (Fig. 1). The overall progression of the two treatments was similar, however, proceeding from a state dominated by ammonium to one more oxidized and comprised mostly of nitrate. The total DIN concentration decreased concurrently with this shift from ammonium- to nitrate-dominance, providing evidence of co-occurring nitrogen loss during the nitrification phase.

Nitrogen loss rates

The rates of anammox and denitrification measured directly in slurries from mesocosm sediments varied with time (Fig. 2). In the low organic matter mesocosms, the denitrification rate was generally higher than the anammox rate (up to ~10 nmol N g^{-1} d^{-1}) but did not fluctuate reproducibly. The anammox rate, however, was consistently low (< 4 nmol N g^{-1} d^{-1}) except for a peak rate of 5 and 8 nmol N g^{-1} d^{-1} in L1 and L2 respectively, toward the end of the incubations. These two mesocosms showed similar trends in the rate time courses, but with a time offset, with L2 lagging L1. This lag was also evident in the DIN concentration time series.

The mesocosms subjected to a high organic matter amendment (Fig. 2C, D) showed a very different trend in the rate measurements. Here, the anammox rates generally were lower than in L1 and showed no significant peak. Further, both H1 and H2 showed dual maxima (up to

20 nmol g^{-1} d^{-1}) in denitrification: one at the beginning of the experiments, just following the organic matter addition, and one toward the end of the incubations. In the previous model analysis, we found that the rates of all biological processes increased in concert with each other, making the percentage of nitrogen loss attributed to anammox consistent regardless of treatment (44.3 ± 0.3% anammox) [5]. From the direct measurements presented here, however, we found the anammox percentages to be lower than the modeled value: 32 ± 8% (SE) for the L mesocosms and 27 ± 8% for the H mesocosms.

Denitrifier nirS and anammox 16S rRNA gene abundances

Because the replication between duplicate mesocosms was very consistent for both treatments, genetic analysis was conducted on sediment DNA extracts from only one mesocosm from each organic treatment, L1 and H1 (Fig. 3). Tank L1 did not show a trend in abundance of the denitrifier *nirS* functional gene, with an average of 6.6 ± 0.4 × 10^7 (SD) gene copies g^{-1} wet sediment. For anammox *16S rRNA*, however, while the total abundance was an order of magnitude lower than *nirS*, there was a significant ~4-fold increase from 2.5 to 10 × 10^6 copies g^{-1} wet sediment between days 10 and 30. This increase in the single copy gene implies a doubling time of 10 days for the anammox community over this time period, similar to previous estimates [51, 52]. The number of gene copies then decreased back toward initial levels. Tank H1 showed the opposite pattern compared with L1: there was no significant trend in the anammox *16S rRNA* gene abundances, averaging 3.5 ± 1.4 × 10^6 copies g^{-1} wet sediment over the time course of the incubation. The denitrifier *nirS* abundance, however, started relatively high (and at the same level as that in L1), approximately 6 × 10^7 copies g^{-1} wet sediment before decreasing until day 16 and then peaking at over 10^8 copies g^{-1} wet sediment on day 38. These

peak abundances in anammox *16S rRNA* in L1 and *nirS* in H1 are significantly greater than the abundances in the remainder of their respective time courses ($p < 10^{-7}$).

Denitrifier community diversity

Based on the denitrification rate and *nirS* gene abundance peaks in H1 at day 38, we investigated whether there was a shift in the community associated with these increases. Such a shift could take the shape of a few dominants or a single winner, or a less obvious change in the overall community composition of the major (> 1% of total) groups. Only 39 of the 164 archetype probes were detected as a major component of at least one sample, and the major groups comprised 66.4%, 54.7%, 46.3%, and 54.0% of the total microarray fluorescence for L1-3, L1-38, H1-3, and H1-38 samples respectively (Fig. 4). These data also show that the major *nirS* community in both treatments at both the beginning (day 3) and near the end (day 38) were not dominated by a single winner. Both Shannon diversity ($H = 3.01 \pm 0.02$) and evenness ($E = 0.95 \pm 0.01$) indices were relatively high and showed little variation across organic matter treatments and time points and indicated a diverse community. However, the community comprising the major groups (those that accounted for > 1% of the total signal) was different among the samples. The Bray-Curtis dissimilarity index (not shown) indicated that the two days sampled from L1 were more similar to each other than to either day in H1, although all four communities were not statistically different due to the abundance of the major groups. H1-3 was most similar to L1-3; and, the most dissimilar samples were L1-38 and H1-38. These results indicate a divergence in community over the 38 days of the incubations caused by the application of labile organic matter.

The composition of the community shift is interesting, and can be delineated based on occurrence in subsets of tanks and times. There were 12 archetypes that represented a major part of the total signal in both tanks at both the beginning and end. Eight of these archetypes represent sequences derived from the Choptank River (Nir71, 5, 134, 115, 82, 33, 150, 112), two from elsewhere in Chesapeake Bay (Nir28, 164), one from the coastal Arabian Sea water column (Nir111), and one (Nir1; *Pseudomonas aeruginosa*) which is found in many environments including Chesapeake Bay sediments and the Arabian Sea oxygen deficient waters [53]. These twelve archetypes comprise a large fraction of the major groups (L1-3: 78%, L1-38: 70%, H1-3: 73%, H1-38: 65%) but, interestingly, account for 8% less of the total after 38 days of incubation with the organic matter amendments.

Upon incubation with a high amount of organic carbon, however, the relative hybridization signal of some groups decreased, and others increased. Archetypes Nir148 and Nir80, which existed in approximately equal proportions at both time points in L1 and in H1-3, and five of the major archetypes in H1-3 were not major components of the community in H1-38. Moreover, eight archetypes, which comprised 18% of that sample's signal, were found only in sample H1-38 (Fig. 4). The most important of these, archetype 123, made up more than 8% of H1-38's signal. This sequence was derived from site CB1 in Chesapeake Bay when/where the measured fixed nitrogen loss rates were highest among all sites analyzed [16]. While the sequence is not closely related to any known organism, it groups with sequences from highly productive systems: Baltic Sea, oxygen deficient zones, and during cyanobacteria blooms [16].

In a principal component analysis of the microarray data, the first two principal components explain 50% and 34% of the variance, respectively (Fig. 5). Samples L1-3 and L1-38 are clustered whereas H1-3 and H1-38 are approximately equidistant from the L1 samples.

The differences between the average of the two L1 samples ($\overline{L1}$) and H1-3 are due to both PC1 and PC2, but $\overline{L1}$ and H1-38 differ only along PC1. The geometric distance in PC1/PC2 space between $\overline{L1}$ and H1-3 is less than that between $\overline{L1}$ and H1-38, confirming the greater similarity between the initial communities in the low and high carbon mesocosms before the addition of organic matter. It is worth noting that the distance between $\overline{L1}$ and H1-3 is in fact less than that between H1-3 and H1-38 (3.9 compared to 4.7), which implies that the divergence of the community during 6 months of pre-incubation was less than the shift observed in the period of 35 days following a large organic carbon amendment. A heatmap based on correlation analysis of the combined RFR, qPCR and environmental data illustrates some relationships among archetypes and other variables. The same archetype clusters are evident in the heatmap (Fig. 6) and the PCA (Fig. 5). For example, *nirS* abundance was positively correlated with the archetype cluster that includes Nir123, one of the archetypes that was significant only in H1 at D38, i.e., in response to the high OM addition. Nir33, which was a significant archetype in the initial samples, was correlated with high DIN concentrations. Nir21 did not cluster with other archetypes but was the archetype with the highest correlation to denitrification rate.

Discussion

Organic matter, as might be derived from a phytoplankton bloom settling event or from seasonal fish farming, induced changes in the nitrogen biogeochemistry observed in the mesocosms. The high OM treatment showed elevated rates of denitrification, as would be expected given the mainly heterotrophic nature of this process and its dependence on organic carbon. Interestingly, however, the response appears bimodal, with the initial peak corresponding to an immediate community response to the labile OM addition, and a second, month-later peak

upon the exhaustion of nitrite and the maximum nitrate concentration in the overlying water. This temporal course of denitrification rates would indicate that the sediment biogeochemistry is such that the denitrifiers will rapidly increase their rates when presented high amounts of labile OM, but a byproduct, either NH_4^+, NO_2^-, or some other unmeasured biomarker, is produced to hinder complete consumption of this OM. When this inhibition is removed, however, the denitrifiers are able to increase their rates again and consume both OM and DIN. In the natural environment, where the overlying water is flushed and replenished, such inhibition may not occur, and the denitrifiers able to consume the organic matter addition much more rapidly.

This inhibition may also encompass competition with DNRA at high levels of dissolved organic matter. As we added particulate organic matter to the pre-incubated mesocosms, there should be a delay in solubilizing this organic amendment and allowing it to build up to levels that thermodynamically favor nitrate reduction to ammonium rather than to N_2 [40, 54, 55]. However, dissolved organic matter levels were not monitored throughout the experiments, and the controls on the partitioning between denitrification and DNRA are more complicated than only organic carbon dependence [56, 57]. Our study does nonetheless imply complex dynamics in the denitrifier population and metabolic rates, and necessitates further investigation into the competition with other microbial communities.

The mesocosm experimental approach allows for the evaluation of how the microbiology responds to an organic matter pulse in the absence of external forcing (e.g., flowing water in the natural system). However, as is often true for sediments, even the mesocosms are subject to heterogeneities and measurement artifacts that obscure the relationships among rates, DIN concentrations, and DNA gene abundances. The peaks in directly measured rates of anammox and denitrification do not consistently correspond either to peaks in the DIN concentrations or to

345 the modeled rates derived from them [5]. There are a number of possible explanations for this
346 discrepancy. First, the discrete rate measurements made once per week may miss actual peaks in
347 the rates. For instance, in the low organic matter mesocosms, small rate maxima that were
348 observed within the first 10 days might have corresponded more precisely to the modeled
349 maximum rate of ammonium consumption at days 8–9 had rate experiments been conducted on
350 those days.

351 Contributing to this lack of overall correlation is the fact that these sediment systems are
352 highly heterogeneous. The labile organic matter amendment was raked over the entire sediment
353 bed, but on the microscale where microbes operate [58], heterogeneities abound. As the systems
354 are driven by the organic material, its distribution is certainly crucial in controlling the small
355 scale locations of biological rates within a sediment matrix. The DIN measurements sampled the
356 homogenous water column overlying the entirety of the sediment bed and integrated the
357 sediment heterogeneity. This led to high reproducibility between duplicate mesocosms in
358 integrated rates modeled from the DIN patterns [5], but rates directly measured in sediment
359 incubations are subject to small scale heterogeneity and therefore less reproducible.

360 The directly measured rates presented here are lower than some literature reports, e.g.,
361 [59–61], but we note that our rates are not directly comparable. Our rates are averaged over the
362 entire 2.5 cm-thick sediment plug whereas the zone of denitrification is likely on the order of
363 one-tenth of that thickness [62]. Accounting for this factor of ten would make the rates reported
364 here on the same order as previous reports in other locations using other methods. Further, the
365 direct rate measurements are consistent with the magnitude of the observed nitrate drawdown.
366 For instance, nitrate was drawn down ~50 μmol L^{-1} in 10 d toward the end of the incubations

(Fig. 1), and given that the mesocosms comprised 2 kg of sediment and 20 L of water, this equates to 50 nmol g^{-1} d^{-1}, again of the same magnitude as the peak rate measurements.

The slurry method used here also meant that the entire sediment column was cored and homogenized in order to minimize artifacts from preferentially selecting only specific depth layers [17]. This homogenization and redistribution of active nitrogen cycle bacteria and organic matter from the interface into the whole core may have altered the proportions of N_2 generation attributed to anammox and denitrification. While the organic matter amendment had a C/N of 4.2, there was a large background C/N of ~9 which is typical of recalcitrant organic matter in estuarine systems [5, 19]. The newly applied organic material was mostly restricted to the active nitrogen loss zone at the sediment water interface which fueled an anammox percentage of ~45% when calculated from the overlying water (see Babbin and Ward [5]). When mixed and redistributed with deeper, more N-depleted organic matter, however, the resulting proportion of anammox was lower, and the average anammox contributions were 32 ± 8% (SE) and 27 ± 8% for the L and H mesocosms, respectively. This is in agreement with previous work [63] showing that slurries tend to favor denitrification when compared with intact sediment cores, especially in highly active sediments.

The measured denitrifier *nirS* and anammox *16S rRNA* gene abundances did not consistently correspond with the instantaneous rates of fixed nitrogen loss. The lack of such a correlation between *nirS* gene abundance with denitrification rates themselves has been seen in other mesocosm experiments seeded with sediments from Eel Pond, Falmouth, MA [17]. There are a number of factors besides presence of particular genes in the DNA that control biological transformation rates and can obscure the relationship between biological rates and the organisms responsible. Particularly, expression of the gene in RNA and substrate availability are important

390 in controlling the actual rates of denitrification. Moreover, homogenization over the whole
391 sediment column can obscure the signal by reducing overall rates and concentrations. Two of the
392 observed abundance maxima, where the signal was strongest, in anammox *16S* genes in L1 at
393 day 27 and *nirS* genes in H1 at day 38 nonetheless did correspond with maxima in directly
394 measured instantaneous rates. The same homogenized sediment slurry that was analyzed for the
395 rates was frozen for DNA extraction, so perhaps during these periods of especially high rates, the
396 signals in gene abundance reflect actual changes in abundance of the relevant microbes. The
397 inhomogeneity of individual sediment cores also likely contributes to lack of direct
398 correspondence between instantaneous rates and gene abundances. It is also very likely that the
399 primers we used did not detect all the members of the two functional groups. It is possible that
400 *nirK* denitrifiers contributed to the rates, but we did not investigate their abundance. The *nirS*
401 gene is very diverse and thus it is likely that some related genes escaped our detection.
402 Regarding anammox gene abundances, Van Kessel et al. [64] found that the dominant anammox
403 phylotype in biofilters in a freshwater aquaculture system was not closely related to known
404 anammox strains and thus would not have been detected with the standard 16S rRNA probes. It
405 is thus possible that anammox abundance detected here by 16S rRNA, was overestimated.
406 The community composition of the major denitrifiers determined from the *nirS*
407 microarray could be interpreted based on presence or absence of a few groups of archetypes. The
408 most abundant taxa were found in all four samples regardless of treatment or day of sampling
409 during the incubation. These 12 important groups derived almost exclusively from Choptank
410 River and Chesapeake Bay sequences and represented up to 52% of the total hybridization
411 signal. Their ubiquity underlines the reason for their importance: these groups exist at the mouth
412 of the Choptank River because they are favored by the environmental variability and conditions

(sediment type, organic matter composition and availability, inorganic nutrient concentrations, and physicochemical factors like salinity) inherent to this location in the estuary. The dominance of only a few archetypes is consistent with previous clone library work from Chesapeake Bay, where only 8 of the 172 detected operational taxonomic units (defined as ≤ 5% dissimilarity) were found to account for 42% of total *nirS* clones [16].

Because of the long pre-incubation before initiating the experiment by making the nutrient additions, it is likely that the microbial assemblage at the first time point had diverged from the natural assemblage in the bay at the time of sampling. Since all four mesocosms were pre-incubated and both sets of treatment replicated very well in terms of net reaction rates [5], the day 3 and day 38 samples are appropriate for investigating the effects of the different organic amendments. In terms of overall community composition, there was no apparent change over the 35 days of mesocosm L1 in that almost all of the major groups that existed at day 3 still existed at day 38. There was a shift in the community in terms of winners and losers from the amendment of high organic matter, however. Near the end of the high organic matter experiment, eight major archetypes that were unique to sample H1-38 and comprised 18% of the total signal were detected. This appearance of new groups in H1 by day 38, and the disappearance of 5 of 6 of the groups unique to H1 on day 3, indicate that minor groups initially undetectable may become important should proper conditions arise. For instance, in this bloom-like scenario, the initially rare archetype Nir123, which was found only in the high organic matter treatment and represented more than 8% of H1-38's total signal, is likely a fast growing group well suited to highly productive conditions. Such dominance of a few denitrifiers responding to episodic environmental changes has also been shown in the Arabian Sea [43]. Archetype Nir123 exemplifies the importance rare taxa may have in transient settings. Without

these otherwise latent groups, sediment systems would not be able to respond as rapidly to pulse-like events such as a settling bloom or anthropogenic discharge, and by extension, could not buffer the coastal sea as readily from eutrophication.

Conclusions

The mesocosm experiments produced results similar to observations reported from the natural Chesapeake Bay setting: greater importance of denitrification in terms of gene abundances and biogeochemical rates compared with anammox, the presence of a small number of highly important groups well-adapted to this system, and the growth of a specific winner under certain eutrophic conditions. Bloom settling events, such as the one simulated here, induce a dynamic cascade of nitrogen cycling processes and the microbial community responsible for these transformations. The transience of a pulse of organic and inorganic nutrients induced a high level of community evolution, stimulating as much divergence in one month as had previously occurred in six months, despite little change in *nirS* gene abundance. Denitrifier functional diversity apparently allows the coastal ecosystem community to adapt quickly and ameliorate the effects of high nutrients and labile organic matter pulses.

This study also implies that the importance of anammox may in fact be underestimated due to the use of the slurry incubation method, and even more importantly, due to the significance of episodic organic loading in estuarine systems. The current paradigm in many coastal systems is that denitrification accounts for upwards of 90% of fixed nitrogen loss [11, 28]. One explanation for this observation is that the high C/N composition of background organic matter [19, 65, 66] favors denitrification without providing a significant ammonium source for anammox. However, given the microbial response to an organic loading event

stimulated in the experiments presented here, periodic blooms should be disproportionately important to both the overall nitrogen loss rates and the partitioning between anammox and denitrification. As the organic matter deposited to the sediments would likely have a greater nitrogen content than the refractory bulk, it is conceivable that the contribution of anammox during times just following deposition and therefore to nitrogen loss as a whole in coastal sediments is greater than previously thought.

Acknowledgements

We thank J. Bowen, J. Cornwell, and M. Owens for assistance in obtaining sediments and site water from Chesapeake Bay, and the UC Davis Stable Isotope Facility for their mass spectrometry measurements. O. Coyle assisted significantly in the sampling of the mesocosms and the tracer experiments. K. Farrell, D. Qiu, and N. Setlur assisted in the nutrient measurements. Funding was provided by a National Defense Science and Engineering Graduate Fellowship to ARB and National Science Foundation grants to BBW. This work was additionally funded by the Princeton Environmental Institute Siebel Energy Grand Challenges Initiative, and by an NSF Postdoctoral Fellowship to ARB (#1402109) during the writing of the manuscript.

476 **References**

477 1. Brandes JA, Devol AH (2002) A global marine-fixed nitrogen isotopic budget:
478 Implications for Holocene nitrogen cycling. Global Biogeochem Cycles 16:1120. doi:
479 10.1029/2001GB001856

480 2. Gruber N (2004) The dynamics of the marine nitrogen cycle and its influence on
481 atmospheric CO_2. In: Follows M, Oguz T (eds) Ocean Carbon Cycle Clim. Kluwer
482 Academic, Dordrecht, pp 97–148

483 3. Codispoti LA (2007) An oceanic fixed nitrogen sink exceeding 400 Tg N a^{-1} vs the
484 concept of homeostasis in the fixed-nitrogen inventory. Biogeosciences 4:233–253.

485 4. Brandes JA, Devol AH (1997) Isotopic fractionation of oxygen and nitrogen in coastal
486 marine sediments. Geochim Cosmochim Acta 61:1793–1801.

487 5. Babbin AR, Ward BB (2013) Controls on Nitrogen Loss Processes in Chesapeake Bay
488 Sediments. Environ Sci Technol 47:4189–4196. doi: 10.1021/es304842r

489 6. Glibert PM, Trice TM, Michael B, Lane L (2005) Urea in the tributaries of the
490 Chesapeake and Coastal Bays of Maryland. Water Air Soil Pollut 160:229–243.

491 7. Lomas MW, Trice TM, Glibert PM, et al. (2002) Temporal and Spatial Dynamics of Urea
492 Uptake and Regeneration Rates and Concentrations in Chesapeake Bay. Estuaries 25:469–
493 482.

494 8. Glibert PM, Harrison J, Heil C, Seitzinger S (2006) Escalating Worldwide use of Urea – A
495 Global Change Contributing to Coastal Eutrophication. Biogeochemistry 77:441–463. doi:
496 10.1007/s10533-005-3070-5

497 9. Christensen PB, Rysgaard S, Sloth NP, et al. (2000) Sediment mineralization, nutrient
498 fluxes, denitrification and dissimilatory nitrate reduction to ammonium in an estuarine
499 fjord with sea cage trout farms. Aquat Microb Ecol 21:73–84.

500 10. Lauer PR, Fernandez M, Fairweather PG, et al. (2009) Benthic fluxes of nitrogen and
501 phosphorus at southern bluefin tuna Thunnus maccoyii sea-cages. Mar Ecol Prog Ser
502 390:251–263.

503 11. Rich JJ, Dale OR, Song B, Ward BB (2008) Anaerobic ammonium oxidation (Anammox)
504 in Chesapeake Bay sediments. Microb Ecol 55:311–320. doi: 10.1007/s00248-007-9277-3

505 12. Koop-Jakobsen K, Giblin AE (2009) Anammox in Tidal Marsh Sediments: The Role of
506 Salinity, Nitrogen Loading, and Marsh Vegetation. Estuaries and Coasts 32:238–245. doi:
507 10.1007/s12237-008-9131-y

13. Braker G, Zhou J, Wu L, et al. (2000) Nitrite Reductase Genes (nirK and nirS) as Functional Markers To Investigate Diversity of Denitrifying Bacteria in Pacific Northwest Marine Sediment Communities. Appl Environ Microbiol 66:2096–2104. doi: 10.1128/AEM.66.5.2096-2104.2000

14. Abell GCJ, Revill AT, Smith C, et al. (2009) Archaeal ammonia oxidizers and nirS-type denitrifiers dominate sediment nitrifying and denitrifying populations in a subtropical macrotidal estuary. ISME J 4:286–300. doi: 10.1038/ismej.2009.105

15. Mosier AC, Francis CA (2010) Denitrifier abundance and activity across the San Francisco Bay estuary. Environ Microbiol Rep 2:667–676. doi: 10.1111/j.1758-2229.2010.00156.x

16. Francis CA, O'Mullan GD, Cornwell JC, Ward BB (2013) Transitions in nirS-type denitrifier diversity, community composition, and biogeochemical activity along the Chesapeake Bay estuary. Front Microbiol 4:237. doi: 10.3389/fmicb.2013.00237

17. Bowen JL, Babbin AR, Kearns PJ, Ward BB (2014) Connecting the dots: Linking nitrogen cycle gene expression to nitrogen fluxes in marine sediment mesocosms. Front Microbiol 5:429. doi: 10.3389/fmicb.2014.00429

18. Smith JM, Mosier AC, Francis CA (2014) Spatiotemporal Relationships Between the Abundance, Distribution, and Potential Activities of Ammonia-Oxidizing and Denitrifying Microorganisms in Intertidal Sediments. Microb Ecol N/A:N/A. doi: 10.1007/s00248-014-0450-1

19. Zimmerman AR, Canuel EA (2001) Bulk organic matter and lipid biomarker composition of Chesapeake Bay surficial sediments as indicators of environmental processes. Estuar Coast Shelf Sci 53:319–341. doi: 10.1006/ecss.2001.0815

20. Middelburg JJ, Soetaert K, Herman PMJ, Heip CHR (1996) Denitrification in marine sediments: A model study. Global Biogeochem Cycles 10:661–673.

21. Cornwell JC, Kemp WM, Kana TM (1999) Denitrification in coastal ecosystems: methods, environmental controls, and ecosystem level controls, a review. Aquat Ecol 33:41–54.

22. Naqvi SWA, Jayakumar DA, Narvekar P V, et al. (2000) Increased marine production of N2O due to intensifying anoxia on the Indian continental shelf. Nature 408:346–349.

23. Dalsgaard T, Thamdrup B, Canfield DE (2005) Anaerobic ammonium oxidation (anammox) in the marine environment. Res Microbiol 156:457–464. doi: 10.1016/j.resmic.2005.01.011

24. Engström P, Penton CR, Devol AH (2009) Anaerobic ammonium oxidation in deep-sea sediments off the Washington margin. Limnol Oceanogr 54:1643–1652. doi: 10.4319/lo.2009.54.5.1643

25. Castine SA, Erler D V, Trott LA, et al. (2012) Denitrification and Anammox in Tropical Aquaculture Settlement Ponds: An Isotope Tracer Approach for Evaluating N_2 Production. PLoS One 7:

26. Minjeaud L, Michotey VD, Garcia N, Bonin PC (2009) Seasonal variation in di-nitrogen fluxes and associated processes (denitrification, anammox and nitrogen fixation) in sediment subject to shellfish farming influences. Aquat Sci 71:425–435.

27. Lisa JA, Song B, Tobias CR, Duernberger KA (2014) Impacts of freshwater flushing on anammox community structure and activities in the New River Estuary, USA. Aquat Microb Ecol 72:17–31.

28. Brin LD, Giblin AE, Rich JJ (2014) Environmental controls of anammox and denitrification in southern New England estuarine and shelf sediments. Limnol Oceanogr 59:851–860. doi: 10.4319/lo.2014.59.3.0851

29. Laanbroek HJ, Gerards S (1993) Competition for limiting amounts of oxygen between Nitrosomonas europaea and Nitrobacter winogradskyi grown in mixed continuous cultures. Arch Microbiol 159:453–459.

30. Kim J-G, Jung M-Y, Park S-J, et al. (2012) Cultivation of a highly enriched ammonia-oxidizing archaeon of thaumarchaeotal group I.1b from an agricultural soil. Environ Microbiol 14:1528–1543. doi: 10.1111/j.1462-2920.2012.02740.x

31. Martens-Habbena W, Berube PM, Urakawa H, et al. (2009) Ammonia oxidation kinetics determine niche separation of nitrifying Archaea and Bacteria. Nature 461:976–979. doi: 10.1038/nature08465

32. Thamdrup B, Dalsgaard T (2002) Production of N2 through Anaerobic Ammonium Oxidation Coupled to Nitrate Reduction in Marine Sediments. Appl Environ Microbiol 68:1312–1318. doi: 10.1128/AEM.68.3.1312-1318.2002

33. Bender M, Jahnke R, Weiss R, et al. (1989) Organic carbon oxidation and benthic nitrogen and silica dynamics in San Clemente Basin, a continental borderland site. Geochim Cosmochim Acta 53:685–697.

34. Kemp WM, Sampou P, Caffrey J, et al. (1990) Ammonium recycling versus denitrification in Chesapeake Bay sediments. Limnol Oceanogr 35:1545–1563. doi: 10.4319/lo.1990.35.7.1545

35. Babbin AR, Keil RG, Devol AH, Ward BB (2014) Organic Matter Stoichiometry, Flux, and Oxygen Control Nitrogen Loss in the Ocean. Science 344:406–408.

36. Trimmer M, Engstrom P (2011) Distribution, activity, and ecology of anammox bacteria in aquatic environments. In: Ward BB, Arp DJ, Klotz MG (eds) Nitrification. ASM Press, Washington, D.C., pp 201–235

37. Dalsgaard T, Canfield DE, Petersen J, et al. (2003) N_2 production by the anammox reaction in the anoxic water column of Golfo Dulce, Costa Rica. Nature 422:606–608. doi: 10.1038/nature01526

38. Caffrey JM, Miller LG (1995) A comparison of two nitrification inhibitors used to measure nitrification rates in estuarine sediments. Fems Microbiol Ecol 17:213–220.

39. Newell RIE, Cornwell JC, Owens MS (2002) Influence of simulated bivalve biodeposition and microphytobenthos on sediment nitrogen dynamics: A laboratory study. Limnol Oceanogr 47:1367–1379.

40. Hardison AK, Algar CK, Giblin AE, Rich JJ (2015) Influence of organic carbon and nitrate loading on partitioning between dissimilatory nitrate reduction to ammonium (DNRA) and N_2 production. Geochim Cosmochim Acta 164:146–160. doi: 10.1016/j.gca.2015.04.049

41. Holmes RM, Aminot A, Kérouel R, et al. (1999) A simple and precise method for measuring ammonium in marine and freshwater ecosystems. Can J Fish Aquat Sci 56:1801–1808.

42. Grasshoff K (1983) Determination of nitrite. In: Grasshoff K, Ehrhardt M, Kremling K (eds) Methods seawater Anal., 2nd ed. Verlag Chemie, Weinheim, pp 143–150

43. Jayakumar A, O'Mullan GD, Naqvi SWA, Ward BB (2009) Denitrifying bacterial community composition changes associated with stages of denitrification in oxygen minimum zones. Microb Ecol 58:350–362.

44. Smith CJ, Nedwell DB, Dong LF, Osborn AM (2006) Evaluation of quantitative polymerase chain reaction-based approaches for determining gene copy and gene transcript numbers in environmental samples. Environ Microbiol 8:804–815. doi: 10.1111/j.1462-2920.2005.00963.x

45. Ward BB, Bouskill NJ (2011) The utility of functional gene arrays for assessing community composition, relative abundance, and distribution of ammonia-oxidizing bacteria and archaea. Methods Enzymol 496:373–396. doi: 10.1016/b978-0-12-386489-5.00015-4

46. Jayakumar A, Peng X, Ward BB (2013) Community composition of bacteria involved in fixed nitrogen loss in the water column of two major oxygen minimum zones in the ocean. Aquat Microb Ecol 70:245–259. doi: 10.3354/ame01654

47. Taroncher-Oldenburg G, Griner EM, Francis CA, Ward BB (2003) Oligonucleotide Microarray for the Study of Functional Gene Diversity in the Nitrogen Cycle in the Environment. Appl Environ Microbiol 69:1159–1171. doi: 10.1128/AEM.69.2.1159-1171.2003

48. Bulow SE, Francis CA, Jackson GA, Ward BB (2008) Sediment denitrifier community composition and nirS gene expression investigated with functional gene microarrays. Environ Microbiol 10:3057–3069. doi: 10.1111/j.1462-2920.2008.01765.x

49. Peng X, Jayakumar A, Ward BB (2013) Community composition of ammonia-oxidizing archaea from surface and anoxic depths of oceanic oxygen minimum zones. Front Microbiol 4:177. doi: 10.3389/fmicb.2013.00177

50. Borcard D, Gillet F, Legendre P (2011) Numerical Ecology with R. Springer, New York

51. Strous M, Heijnen JJ, Kuenen JG, Jetten MSM (1998) The sequencing batch reactor as a powerful tool for the study of slowly growing anaerobic ammonium-oxidizing microorganisms. Appl Microbiol Biotechnol 50:589–596.

52. Van der Star WRL, van de Graaf MJ, Kartal B, et al. (2008) Response of Anaerobic Ammonium-Oxidizing Bacteria to Hydroxylamine. Appl Environ Microbiol 74:4417–4426. doi: 10.1128/AEM.00042-08

53. Jayakumar DA, Francis CA, Naqvi SWA, Ward BB (2004) Diversity of nitrite reductase genes (nirS) in the denitrifying water column of the coastal Arabian Sea. Aquat Microb Ecol 34:69–78.

54. Porubsky WP, Weston NB, Joye SB (2009) Benthic metabolism and the fate of dissolved inorganic nitrogen in intertidal sediments. Estuar Coast Shelf Sci 83:392–402. doi: 10.1016/j.ecss.2009.04.012

55. Algar CK, Vallino JJ Predicting microbial nitrate reduction pathways in coastal sediments. Aquat Microb Ecol 71:223–238.

56. Kraft B, Tegetmeyer HE, Sharma R, et al. (2014) The environmental controls that govern the end product of bacterial nitrate respiration. Science 345:676–9. doi: 10.1126/science.1254070

57. Behrendt A, Tarre S, Beliavski M, et al. (2014) Effect of high electron donor supply on dissimilatory nitrate reduction pathways in a bioreactor for nitrate removal. Bioresour Technol 171:291–297. doi: 10.1016/j.biortech.2014.08.073

58. Stocker R (2012) Marine Microbes See a Sea of Gradients. Science 338:628–633. doi: 10.1126/science.1208929

59. Joye SB, Smith S V., Hollibaugh JT, Paerl HW (1996) Estimating denitrification rates in estuarine sediments: A comparison of stoichiometric and acetylene based methods. Biogeochemistry 33:197–215. doi: 10.1007/BF02181072

60. Teixeira C, Magalhães C, SB J, A BA (2012) Potential rates and environmental controls of anaerobic ammonium oxidation in estuarine sediments. Aquat Microb Ecol 66:23–32.

61. Song GD, Liu SM, Marchant H, et al. (2013) Anammox, denitrification and dissimilatory nitrate reduction to ammonium in the East China Sea sediment. Biogeosciences 10:6851–6864. doi: 10.5194/bg-10-6851-2013

62. Risgaard-Petersen N, Nicolaisen MH, Revsbech NP, Lomstein BA (2004) Competition between ammonia-oxidizing bacteria and benthic microalgae. Appl Environ Microbiol 70:5528–37. doi: 10.1128/AEM.70.9.5528-5537.2004

63. Trimmer M, Risgaard-Petersen N, Nicholls JC, Engström P (2006) Direct measurement of anaerobic ammonium oxidation (anammox) and denitrification in intact sediment cores. Mar Ecol Prog Ser 326:37–47.

64. Van Kessel MAHJ, Harhangi HR, van de Pas-Schoonen K, et al. (2010) Biodiversity of N-cycle bacteria in nitrogen removing moving bed biofilters for freshwater recirculating aquaculture systems. Aquaculture 306:177–184.

65. Matson EA, Brinson MM (1990) Stable carbon isotopes and the C:N ratio in the estuaries of the Pamlico and Neuse Rivers, North Carolina. Limnol Oceanogr 35:1290–1300.

66. Law CS, Rees AP, Owens NJP (1991) Temporal variability of denitrification in estuarine sediments. Estuar Coast Shelf Sci 33:37–56.

Figure legends

Fig. 1. DIN time series. (A) L1 (filled symbols), L2 (open symbols) and (B) H1 (filled symbols), H2 (open symbols). Ammonium measurements are in blue, nitrite in green, and nitrate in red. Black line denotes the sum of these nitrogen nutrients. Error bars show reproducibility of duplicate measurements. Figure is modified from Babbin and Ward (5).

Fig. 2. Instantaneous rates of anammox and denitrification. (A) L1, (B) L2, (C) H1, (D) H2. Anammox rates are shown in blue and denitrification in red. Error bars represent standard error on slopes through labeled N_2 measurements.

Fig. 3. DNA gene abundances throughout the experiment. *Anammox 16S* (black) and *nirS* (grey) abundance time courses are shown for (A) L1 and (B) H1 mesocosms. Error bars show standard deviations among triplicate PCR amplifications.

Fig. 4. Relative *nirS* abundances. Stacked bar plot of *nirS* microarray RFRs. Purple = found in both L1 and H1; Red = unique to L1; Green = unique to H1; Blue = found only in H1–38; orange/yellow = in all but H1–38. Numbers indicate important archetype probes.

Fig. 5. PCA of *nirS* microarray analysis. A PCA plot of *nirS* probe abundances (indicated by superimposed numbers) for each of the 4 samples. The same color coding is used as in Fig. 4.

Fig. 6. Heatmap similarities among probes and metadata. The heatmap shows how certain archetype probes and environmental metadata (i.e., DIN concentrations, gene abundances, and measured rates) relate to each other. The sequence of red boxes along the diagonal indicates groups of highly related variables.

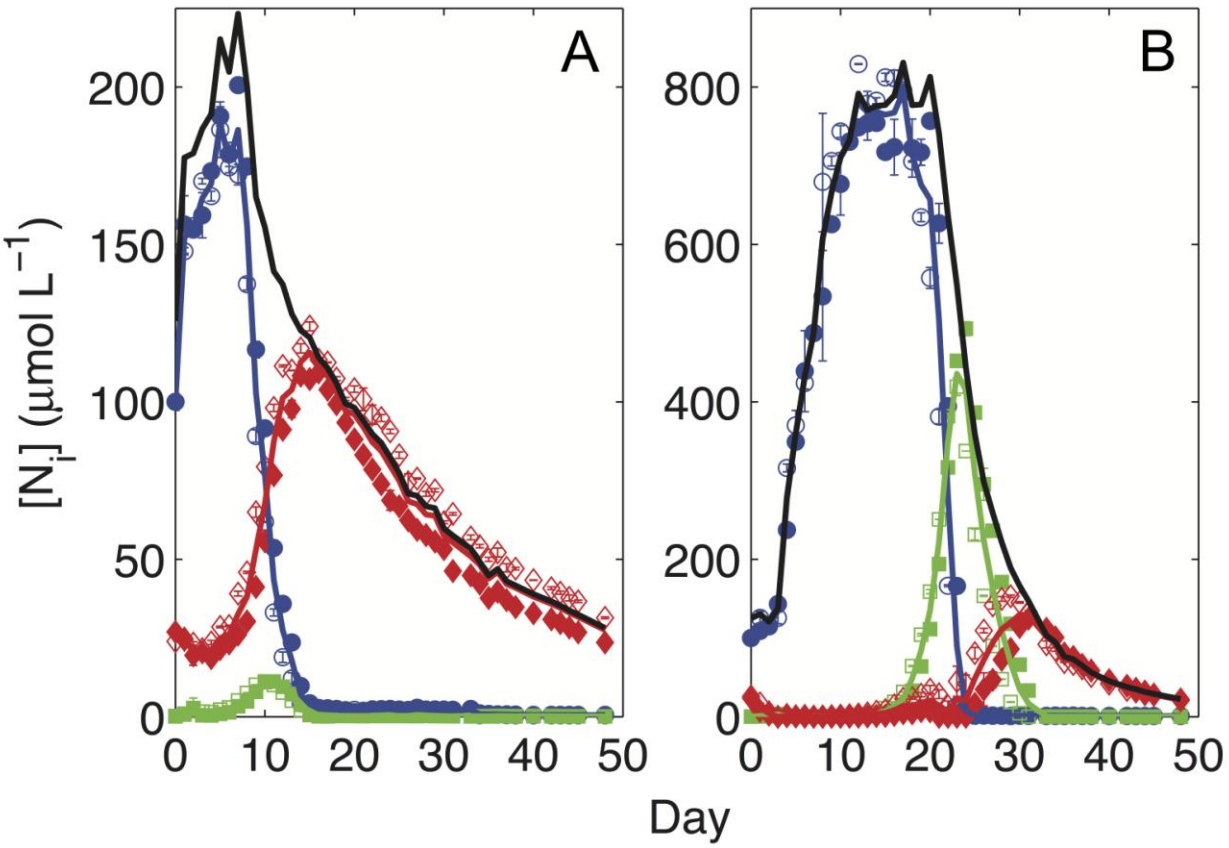

691

692 **Fig. 1. DIN concentrations time series.** (A) Mesocosms L1 (filled symbols), L2 (open symbols)
693 and (B) Mesocosms H1 (filled symbols), H2 (open symbols). Ammonium measurements are in
694 blue, nitrite in green, and nitrate in red. Black line denotes the sum of these nitrogen nutrients.
695 Error bars show reproducibility of duplicate measurements. Figure is modified from Babbin and
696 Ward (5).

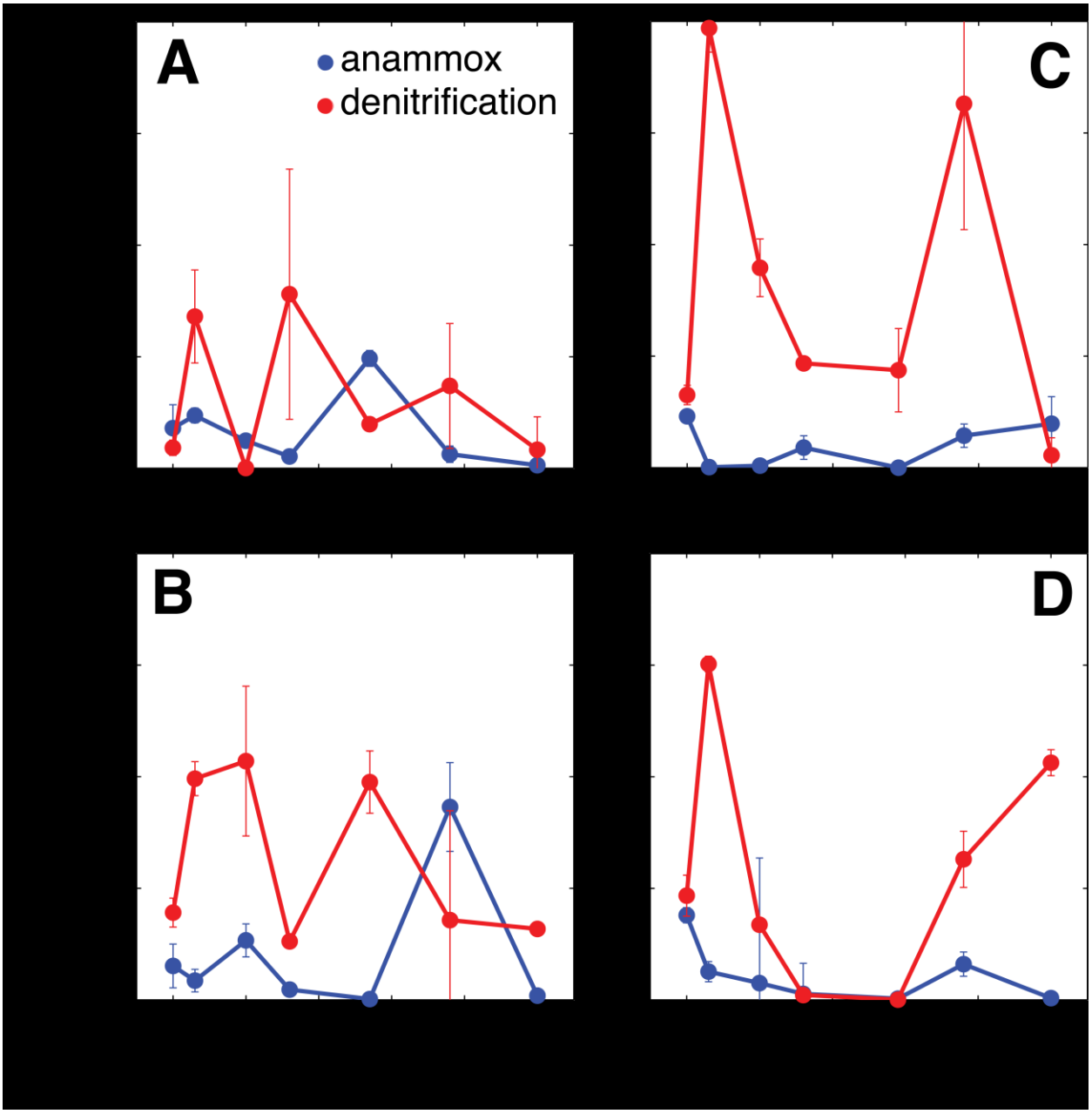

Fig. 2. Instantaneous rates of anammox and denitrification. (A) L1, (B) L2, (C) H1, (D) H2. Anammox rates are shown in blue and denitrification in red. Error bars represent standard error on slopes through labeled N_2 measurements.

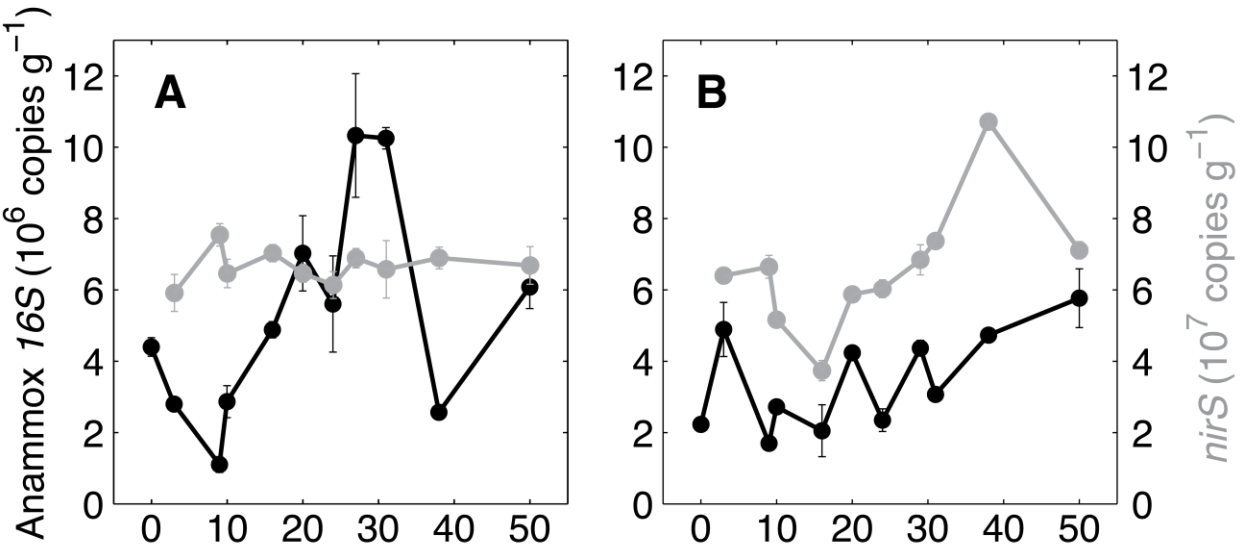

Fig. 3. DNA gene abundances throughout the experiment. *Anammox 16S* (black) and *nirS* (grey) abundance time courses are shown for (A) L1 and (B) H1 mesocosms. Error bars show standard deviations among triplicate PCR amplifications.

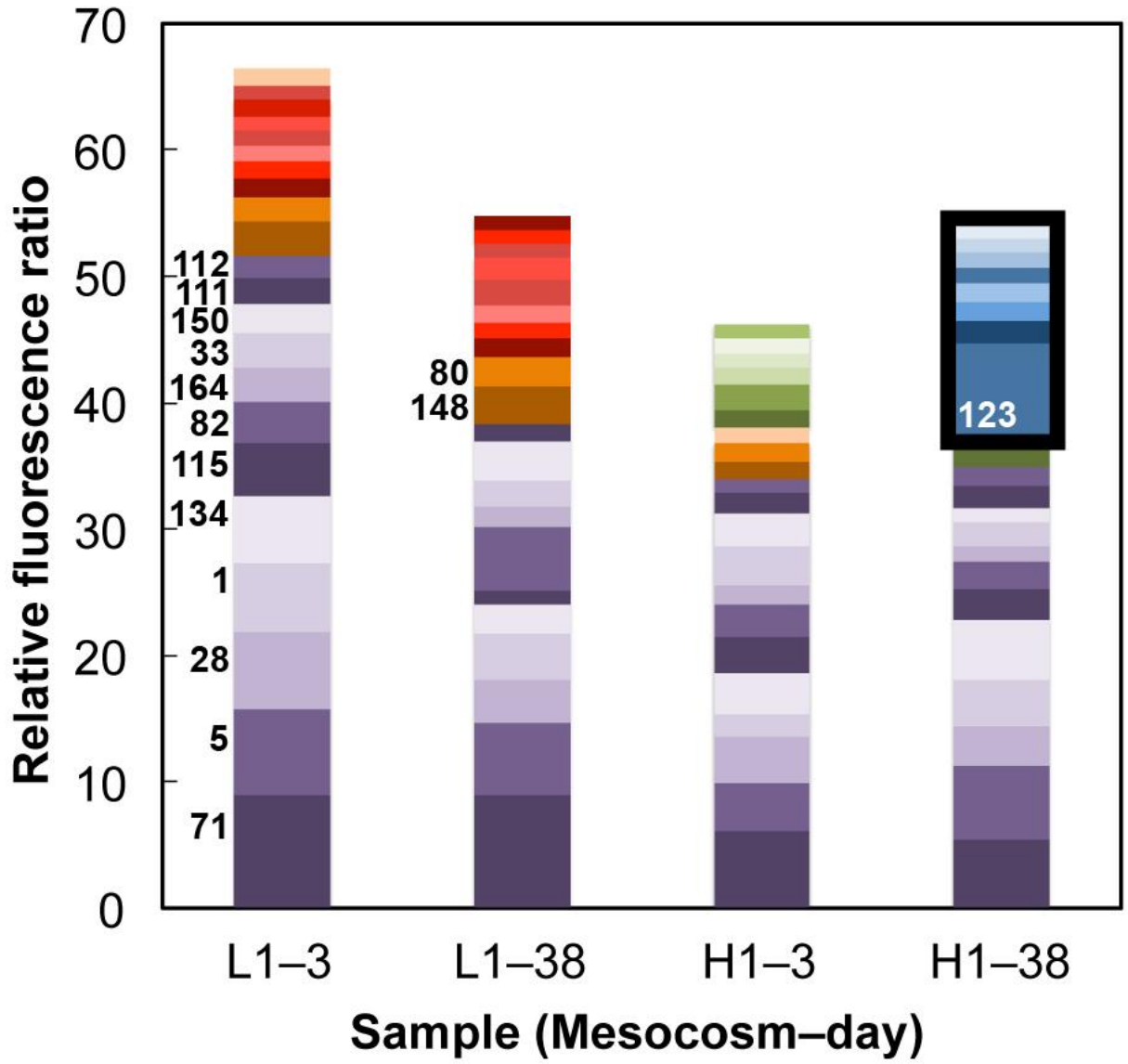

705

706 **Fig. 4. Relative *nirS* abundances.** Stacked bar plot of *nirS* microarray RFRs. Purple = found in

707 both L1 and H1; Red = unique to L1; Green = unique to H1; Blue = found only in H1–38;

708 orange/yellow = in all but H1–38. Numbers indicate important archetype probes.

709

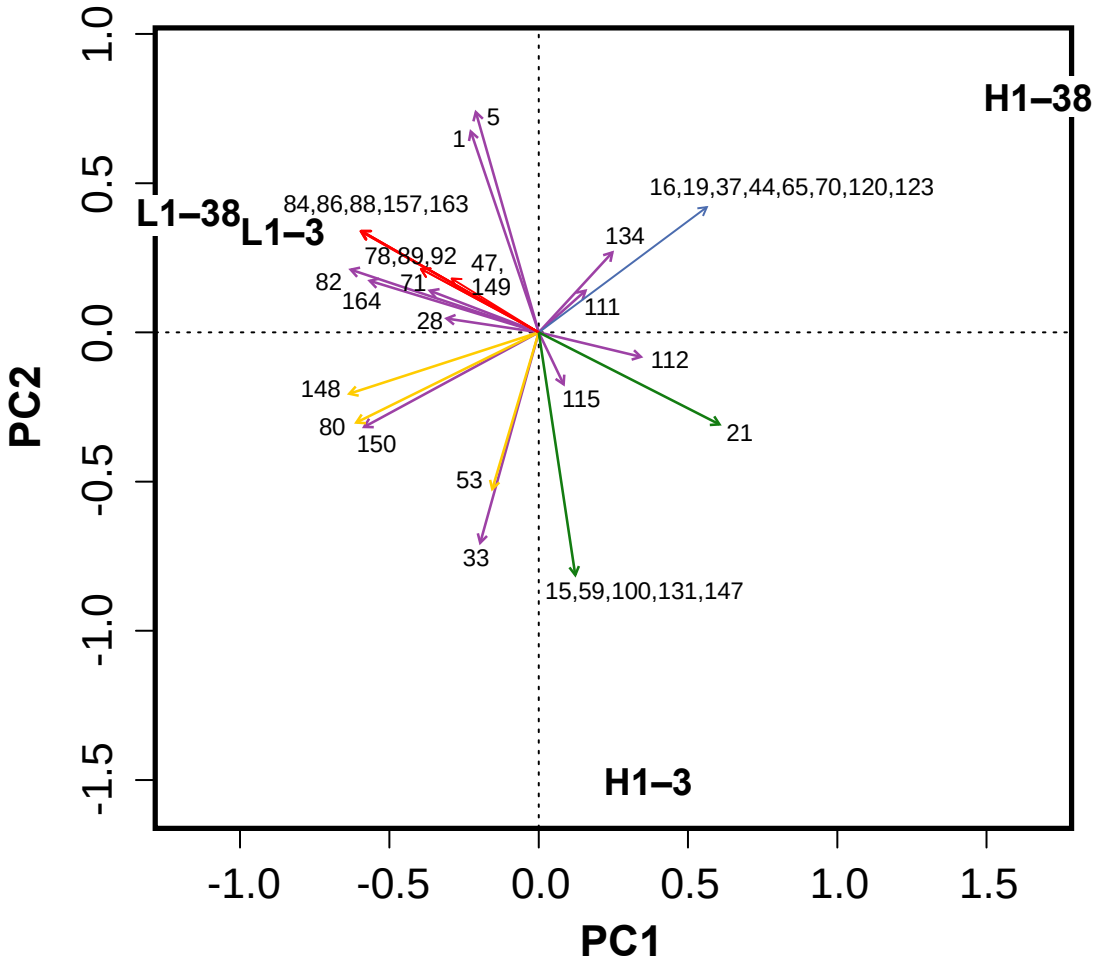

710

711 **Fig. 5. PCA of *nirS* microarray analysis.** A PCA plot of *nirS* probe abundances (indicated by

712 superimposed numbers) for each of the 4 samples. The same color coding is used as in Fig. 4.

713

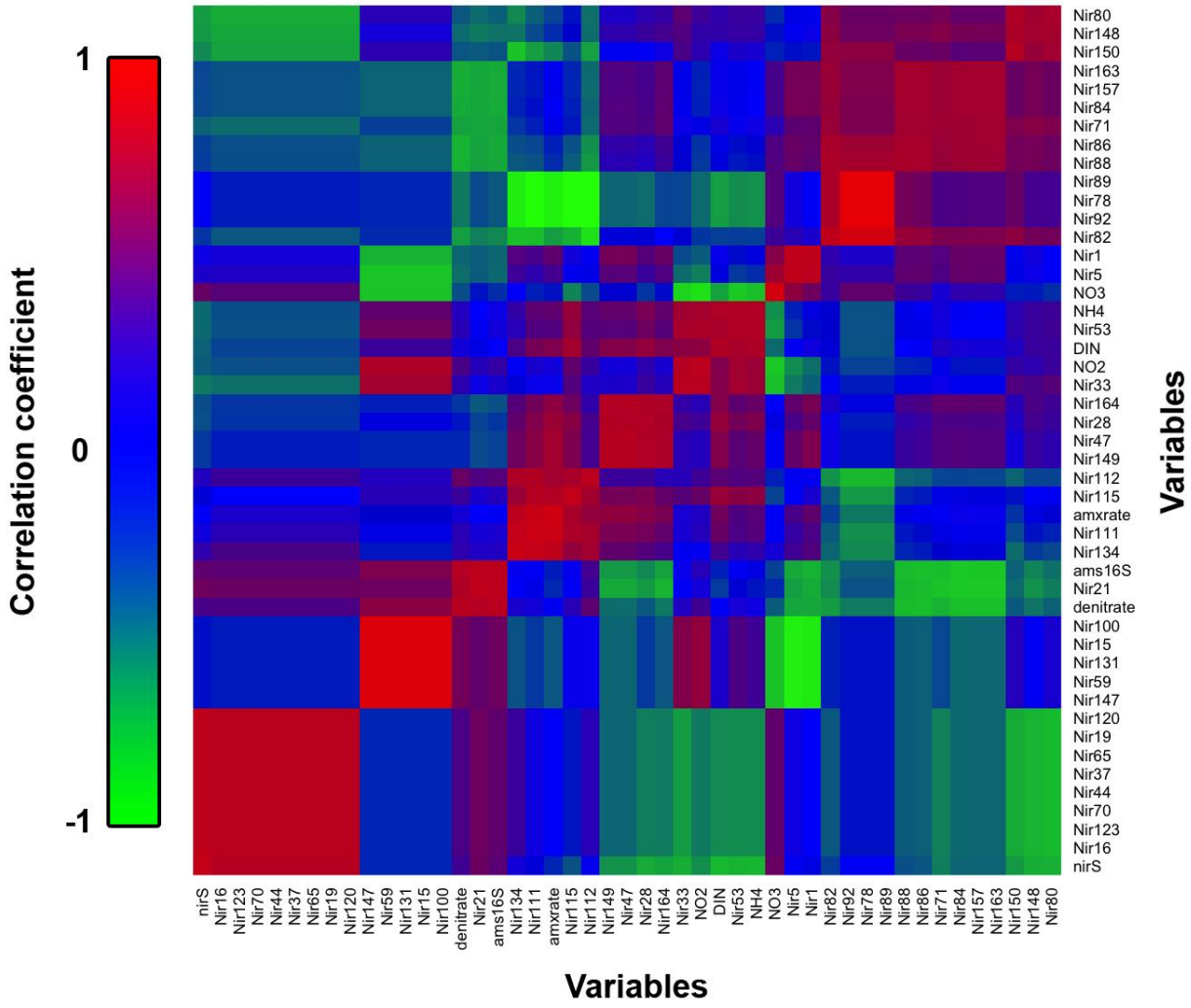

714

715 **Fig. 6. Heatmap similarities among probes and metadata.** The heatmap shows how certain

716 archetype probes and environmental metadata (i.e., DIN concentrations, gene abundances, and

717 measured rates) relate to each other. The sequence of red boxes along the diagonal indicates

718 groups of highly related variables.